FORWARD KINEMATICS AND GEOMETRIC CONTROL OF A MEDICAL ROBOT

Application to Dental Implantation

Richard Chaumont, Eric Vasselin and Dimitri Lefebvre
GREAH of LE HAVRE University, 25 rue Philippe LEBON. 76058 LE HAVRE Cede, France

Keywords: Surgical robotics, geometric modelling, inverse geometric modelling, dynamic modelling, non linear system, identification.

Abstract: Recently, robotics has found a new field of research in surgery in which it is used as an assistant of the surgeon in order to promote less traumatic surgery and minimal incision of soft tissue. In accordance with the requirements of dental surgeons, we offer a robotic system dedicated to dental implants. A dental implant is a mechanical device fixed into the patient's jaw. It is used to replace a single tooth or a set of missing teeth. Fitting the implant is a difficult operation that requires great accuracy. This work concerns the prototype of a medical robot. Forward and inverse kinematics as dynamics are considered in order to drive a control algorithm which is as accurate and safe as possible.

1 INTRODUCTION

Computer-assisted dental implantology is a multidisciplinary and complex topic that includes medical imagery, robotics and computer vision (Langlotz, & *al*, 2000 ; Nikou & *al*, 2000). The fitting of a dental implant is currently the only technique suitable to permanently restore the teeth. For this purpose, specific surgery has been recently developed. Such operations require great accuracy. Moreover, the spread of this type of surgery justifies the extension and use of new techniques (Taylor, 1994). This research and development work focuses on the medical robotics applied to dental implantology. The main contributions of this article are to discuss the forward kinematics and kinematics uncertainties, and also to provide a geometric control for the orientation of the drill.

2 MEDICAL ROBOTICS

For the last twenty years, new technologies have been used to improve surgical operations so that medical research and engineering improvements are closely linked today. On one hand, data processing, computer vision and medical imaging are used in an intensive way in operation rooms. On the other hand, the three principles of robotics-perception, reasoning and action - have been adapted for medical and surgery issues (Lavallee & *al*, 1995). The main goal is to bring together the fundamental principles of robotics and computer vision in order to assist the surgeon in daily therapeutic operations. The aims of medical robotics are to provide less traumatic investigation systems, to provide simulation tools, and, finally, to provide tools that are easier and more flexible to use.

The aim of dental implantology is to use bones and implants in order to provide prosthetic support. The main advantage in comparison with a conventional prosthesis is that dental implantology doesn't mutilate healthy teeth. At the time tooth extraction is completed, the fitting of a dental implant allows the consolidation of the prostheses. The main difficulty is to place the implants correctly. That is the reason why conventional prosthesis is still prefered to dental implantology in many cases.

Dental implants guarantee the patient better comfort but can also reduce overall cost owing to their longevity and lack of inherent complications in comparison with classic prostheses. For difficult cases (completely toothless patients, weak density bones, multiple implants, etc), dental surgeons are confronted with a complex operation. Over the years, the main difficulty concerned the integration of the bone-implant.

This problem has been solved by technical improvements and surgical advances (equipment, implant shapes, surgical protocol, etc). According to

Chaumont R., Vasselin E. and Lefebvre D. (2007).
FORWARD KINEMATICS AND GEOMETRIC CONTROL OF A MEDICAL ROBOT - Application to Dental Implantation.
In *Proceedings of the Fourth International Conference on Informatics in Control, Automation and Robotics*, pages 110-115
DOI: 10.5220/0001652501100115

the opinion of many clinicians, the difficulty is henceforth to improve fitting techniques. The position and orientation of implants must take into account biomechanical and anatomical constraints (Dutreuil, 2001) involving three main criteria: mastication, phonetics and aesthetics. In particular, the problems to be solved are :

- How to adjust the implant position in the correct axis.
- How to optimize the relative position of two adjacent implants.
- How to optimize the implant position according to the bone density.
- How to conduct minimal incision of soft tissue.

Our answer to these questions is image guided surgery (Etienne & *al*, 2000). This solution uses an optical navigation system with absolute positioning in order to obtain position and orientation of the surgeon's tool in real time with respect to the patient's movements. The operation is planned on the basis of scanner data or x-ray images for simple clinical cases.

Figure 1: Navigation system.

The technique consists in initializing the superimposing of patient data and data derived form a set of specific points attached to the patient's jaw (Granger, 2003). The patient's jaw is then analyzed in real time by the navigation system. The Dental View navigation machine guides the surgeon via the image during the operative phase.

However, clinical tests show that supplementary assistance is necessary to help the surgeon during the drilling phase in order to fulfil precision requirements. For this purpose, we developed a surgical robot which controls orientation during the drilling phase.

Our robot is a semi-active mechanical device. It has a passive arm and a motorized wrist with three degrees of freedom (dof) that are not convergent (i.e. not a spherical wrist). The basis is passive, that is to say it is not motorized and can be manipulated by the surgeon like an instrument. The aim of the controller is to guide the surgeon so that it will respect the scheduled orientation.

3 FORWARD KINEMATICS

Drill orientation is characterized by 3 dof RotY, RotX and RotZ and depends also on contra angle ca (Fig. 3). The structure is represented in Fig.2.

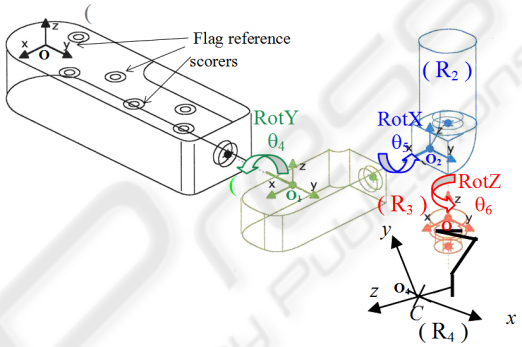

Figure 2: Robot axis.

3.1 Notations

We use homogeneous transformations to describe position and orientation from one link to another. Let us consider the matrix M :

$$M = \begin{bmatrix} R & T \\ P & Q \end{bmatrix} \quad (1)$$

with P = [0 0 0], Q = [1] is a homothetic coefficient equal to 1 (orthogonal transformation); R is a orthogonal rotation matrix; and T is a translation matrix.

For simplicity, calculations are not given in detail. Notations will be represented above Fig.3.

Lxo, Lyo, Lzo : distance x, y, z between computer vision coordinate frame and 4th joint coordinate frame.
Lx5, Lz6 : distance x, z between 4th joint and 5th joint.
Lyca, Lzca : distance y, z between 5 th joint and effector.
Lztool : drill length.
θ_4, θ_5, θ_6 : wrist joint variables.
Ca: contra angle.
ε_i: orthogonal uncertainty between joints.
l_i: length uncertainty between links.

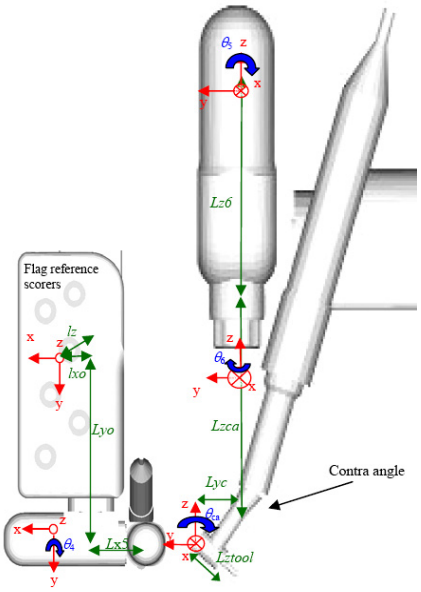

Figure 3: Robot parameters and axes.

3.2 Kinematic Uncertainties

First, we are going to determine the effector position in the ideal case, without considering uncertainties related to length and orthogonality links. We use homogeneous transformations to change the coordinate frame attached to a joint to the coordinate frame attached to the next one. We obtain 6 matrices that change the coordinate frames according to (2) :

$$A_1=\begin{pmatrix}1&0&0&Lxo\\0&1&0&Lyo\\0&0&1&Lzo\\0&0&0&1\end{pmatrix}\ A_2=\begin{pmatrix}\cos\theta_4&0&\sin\theta_4&0\\0&1&0&0\\-\sin\theta_4&0&\cos\theta_4&0\\0&0&0&1\end{pmatrix}\ A_3=\begin{pmatrix}1&0&0&Lx5\\0&\cos\theta_5&-\sin\theta_5&0\\0&\sin\theta_5&\cos\theta_5&0\\0&0&0&1\end{pmatrix}$$
$$A_4=\begin{pmatrix}\cos\theta_6&-\sin\theta_6&0&0\\\sin\theta_6&\cos\theta_6&0&0\\0&0&1&Lz6\\0&0&0&1\end{pmatrix}\ A_5=\begin{pmatrix}1&0&0&0\\0&\cos(ca)&-\sin(ca)&0\\0&\sin(ca)&\cos(ca)&0\\0&0&0&1\end{pmatrix}\ A_6=\begin{pmatrix}1&0&0&0\\0&1&0&Lyca\\0&0&1&Lzca\\0&0&0&1\end{pmatrix} \quad (2)$$

Ideal position in flag coordinate frame results from the preceding matrices :

$$V_{ideal}(R_0)=A_1\times A_2\times A_3\times A_4\times A_5\times A_6\times V(R_4) \quad (3)$$

with $V(R_4) = [0\ 0\ 1\ 0]^T$ to get effector orientation for the "z" axis and $V(R_4) = [0\ 0\ 0\ 1]^T$ to get effector position.

$$A_1^{'}=\begin{pmatrix}1&0&0&Lxo\pm l_{xo}\\0&1&0&Lyo\pm l_{yo}\\0&0&1&Lzo\pm l_{zo}\\0&0&0&1\end{pmatrix}$$

$$A_2^{'}=\begin{pmatrix}1&0&0&0\\0&\cos\pm\varepsilon_1&-\sin\pm\varepsilon_1&0\\0&\sin\pm\varepsilon_1&\cos\pm\varepsilon_1&0\\0&0&0&1\end{pmatrix}\times\begin{pmatrix}\cos\theta_4&0&\sin\theta_4&0\\0&1&0&0\\-\sin\theta_4&0&\cos\theta_4&0\\0&0&0&1\end{pmatrix}\times\begin{pmatrix}\cos\pm\varepsilon_2&-\sin\pm\varepsilon_2&0&0\\\sin\pm\varepsilon_2&\cos\pm\varepsilon_2&0&0\\0&0&1&0\\0&0&0&1\end{pmatrix}$$
$$A_3^{'}=\begin{pmatrix}1&0&0&Lx5\pm l_{x5}\\0&\cos\theta_5&-\sin\theta_5&0\\0&\sin\theta_5&\cos\theta_5&0\\0&0&0&1\end{pmatrix}\times\begin{pmatrix}\cos\pm\varepsilon_3&0&\sin\pm\varepsilon_3&0\\0&1&0&0\\-\sin\pm\varepsilon_3&0&\cos\pm\varepsilon_3&0\\0&0&0&1\end{pmatrix}\times\begin{pmatrix}\cos\pm\varepsilon_4&-\sin\pm\varepsilon_4&0&0\\\sin\pm\varepsilon_4&\cos\pm\varepsilon_4&0&0\\0&0&1&0\\0&0&0&1\end{pmatrix}$$
$$A_4^{'}=\begin{pmatrix}1&0&0&0\\0&\cos\pm\varepsilon_5&-\sin\pm\varepsilon_5&0\\0&\sin\pm\varepsilon_5&\cos\pm\varepsilon_5&0\\0&0&0&1\end{pmatrix}\times\begin{pmatrix}\cos\pm\varepsilon_6&0&\sin\pm\varepsilon_6&0\\0&1&0&0\\-\sin\pm\varepsilon_6&0&\cos\pm\varepsilon_6&0\\0&0&0&1\end{pmatrix}\times\begin{pmatrix}\cos\theta_6&-\sin\theta_6&0&0\\\sin\theta_6&\cos\theta_6&0&0\\0&0&1&Lz6\pm l_{z6}\\0&0&0&1\end{pmatrix}$$
$$A'5=\begin{pmatrix}1&0&0&0\\0&1&0&Lyca\pm l_{yca}\\0&0&1&Lzca\pm l_{zca}\\0&0&0&1\end{pmatrix}$$
$$A_6^{'}=\begin{pmatrix}1&0&0&0\\0&\cos(ca)&-\sin(ca)&0\\0&\sin(ca)&\cos(ca)&0\\0&0&0&1\end{pmatrix}\times\begin{pmatrix}\cos\pm\varepsilon_5&0&\sin\pm\varepsilon_5&0\\0&1&0&0\\-\sin\pm\varepsilon_5&0&\cos\pm\varepsilon_5&0\\0&0&0&1\end{pmatrix}\times\begin{pmatrix}\cos\pm\varepsilon_6&-\sin\pm\varepsilon_6&0&0\\\sin\pm\varepsilon_6&\cos\pm\varepsilon_6&0&0\\0&0&1&0\\0&0&0&1\end{pmatrix} \quad (4)$$

We will model actual position and orientation of the effector by considering uncertainties relating to link length (maximum tolerance of 0.1 mm) and also of frame orthogonal uncertainties (maximum tolerance 0.1 degree). Because of digital encoder resolution (200 000 points per revolution) and of gear reduction encoders uncertainties are negligible.

Moreover, we only consider uncertainties that concern the robot wrist (the arm is a passive mechanical structure). For every dof two uncertainty matrices are added according to the axes that are not articulated. Equation (4) is obtained as a consequence.

Actual effector position is given by (5):

$$V_{actual}(R_0)=A'_1\times A'_2\times A'_3\times A'_4\times A'_5\times A'_6\times V(R_4) \quad (5)$$

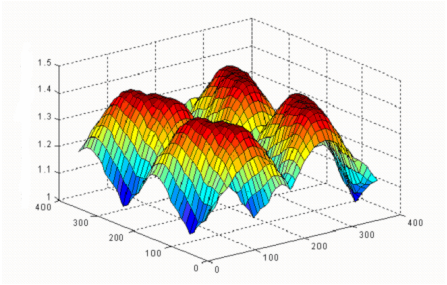

Figure 4: Magnitude of error function for θ_4 and θ_5.

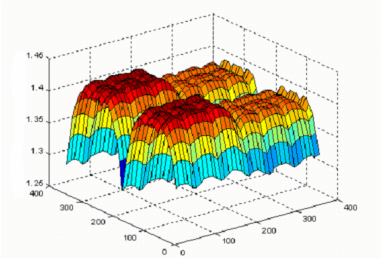

Figure 5: Magnitude of error function for θ_4 and θ_6.

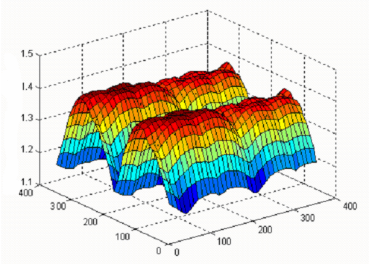

Figure 6: Magnitude of error function for θ_5 and θ_6.

From (4) and (5), we know the ideal position and orientation of the wrist as well as its actual position and orientation which take kinematic uncertainties into account. Therefore, we can obtain the position and orientation errors :

$$E(R_0) = V_{actual}(R_0) - V_{ideal}(R_0) \quad (6)$$

Figs. 4 to 6 represent the maximal uncertainty magnitude (millimeter) generated by mechanical and assembly tolerances. One observes that :

- Uncertainty magnitude is always superior to 1 millimeter,
- Uncertainty magnitude can reach 1.4 millimeters for particular link positions.

In order to fulfil precision requirements uncertainties must be lower than 1 millimeter. Therefore, it is necessary to calibrate the robot wrist.

4 DYNAMICS

In this section we will propose a dynamic model for the axis of the robot. The axis control architecture is presented in Fig.7. Technical caracteristics of the electromechanical and electronic devices can be found in (Chaumont & *al*, 2006).

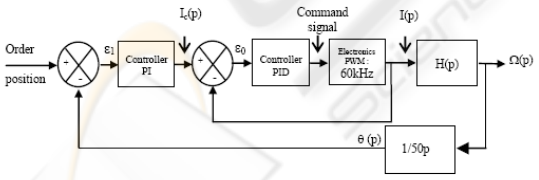

Figure 7: Axis control structure.

4.1 Identification of Electromechanical Device

Closed loop identification for electromechanical device is proposed in this section (Richalet, 1998). System output is the velocity and system input is the current. The robot axis has been placed so that inertia moment can be considered as constant whatever the orientation.

The time response (Fig. 8) presents a dissymmetry between the current generating the acceleration in comparison with the current generating the deceleration.

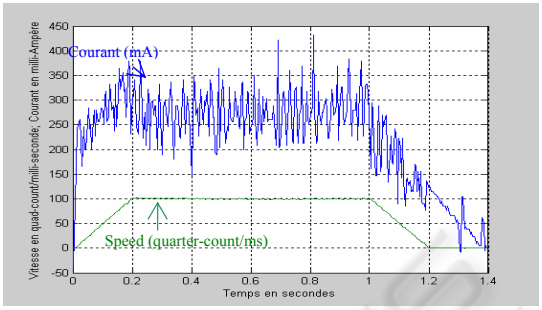

Figure 8: Protocol signature.

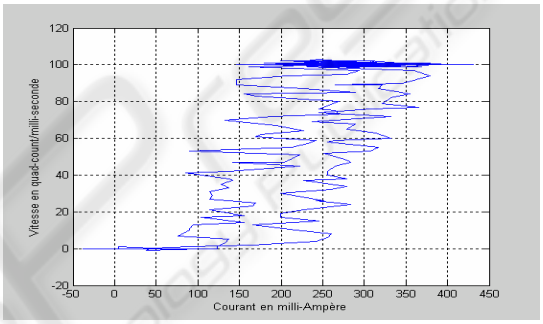

Figure 9: Hysteresis system.

The process is non linear. Fig. 9 represents input/output signature with a dead zone and a histereses. The electromechanical transfer function is represented in Fig.13.

4.2 Identification of Electronic Device

Electronic device input is the desired current and output is the actual current. It represents the electronic system part that is composed of the PWM and its controller.

Identification is achieved in closed loop. A survey of electronic control shows us that the transfer function is a second order overshoot with a stable zero.

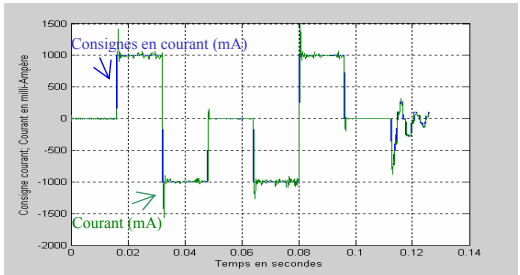

Figure 10: Protocol signature.

4.3 Discussion

The model is validated with the same desired current. Results obtained with the model and with the system are compared according to velocity kinetics (Fig. 11) and position (Fig. 12).

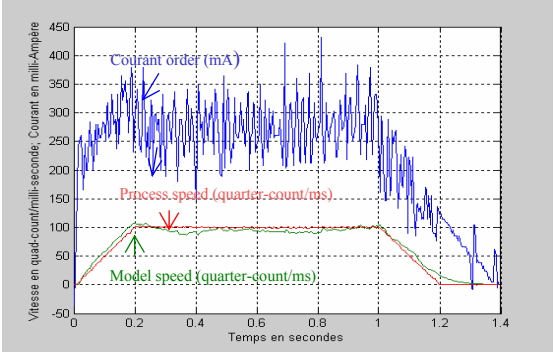

Figure 11: Velocity response.

Parameters

$\omega_0 = 730.97$; $\xi = 0.4258$; $K = 0.9955$; $k = 0.5969$; $T = 0.539$

Histereses size: 75 mA Dead zone size: 115 mA.

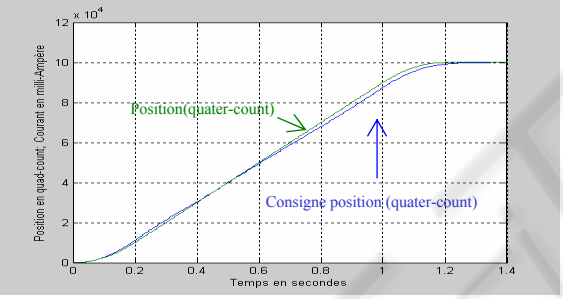

Figure 12: Position response.

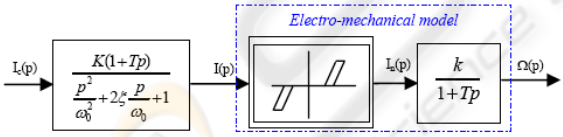

Figure 13: Axis module.

5 CONTROL DESIGN

Forward kinematics is given by equation (2). This model shows how to determine the effector's position and orientation in terms of the joint variables with a function "f". Inverse kinematics is concerned with the problem of finding the joint variables in terms of effector's position and orientation. Our aim is to control the orientation of the effector. The function "f" corresponds therefore to $V_{ideal}\ (R_0)$ expressed by equation (3) with $V(R_4) = [0\ 0\ 1\ 0]^T$ (uncertainties are not considered for control design).

Matrix $V_{ideal}\ (R_0)$ leads to equations (7) to (9) :

$$Vx_0=\sin(ca).\cos(\theta_4).\sin(\theta_6)-\sin(ca).\sin(\theta_4).\sin(\theta_5).\cos(\theta_6)+\sin(\theta_4).\cos(\theta_5).\cos(ca) \quad (7)$$

$$Vy_0 = -\cos(\theta_5).\cos(\theta_6).\sin(ca) - \sin(\theta_5).\cos(ca) \quad (8)$$

$$Vz_0 = -\sin(ca).\sin(\theta_4).\sin(\theta_6) - .\cos(\theta_4).\sin(\theta_5).\cos(\theta_6) + \cos(\theta_4).\cos(\theta_5).\cos(ca) \quad (9)$$

From equations (7), (8) and (9), expressions θ_4, θ_5 and θ_6 are determined.

$$\theta_6 = \text{asin}\ \frac{\cos(\theta_4).Vx_0 - \sin(\theta_4).Vz_0}{\sin(ca)}\ ,\ \theta_{6a} = \pi - \theta_6 \quad (10)$$

$$\theta_5 = \text{acos}\left(\frac{Vy_0}{\rho_1}\right) + a_1\ ,\ \theta_{5a} = -\text{acos}\left(\frac{Vy_0}{\rho_1}\right) + 2.a_1 \quad (11)$$

with : $\rho_1 = \sqrt{(\cos(\theta_6).\sin(ca))^2 + \cos^2(ca)}$

$$a_1 = \text{atan}\left(\frac{\cos(ca)}{\cos(\theta_6).\sin(ca)}\right) + \pi \quad \text{if } -\cos(\theta_6).\sin(ca) < 0$$

$$\text{or } a_1 = \text{atan}\left(\frac{\cos(ca)}{\cos(\theta_6).\sin(ca)}\right) \quad \text{if } -\cos(\theta_6).\sin(ca) > 0$$

$$\theta_{5b} = \text{acos}\left(\frac{Vy_0}{\rho_2}\right) + a_2\ ,\ \theta_{5c} = -\text{acos}\left(\frac{Vy_0}{\rho_2}\right) + 2.a_2 \quad (12)$$

with : $\rho_2 = \sqrt{(\cos(\theta_{6a}).\sin(ca))^2 + \cos^2(ca)}$

$$a_2 = \text{atan}\left(\frac{\cos(ca)}{\cos(\theta_{6a}).\sin(ca)}\right) + \pi \quad \text{if } -\cos(\theta_{6a}).\sin(ca) < 0$$

$$\text{or } a_2 = \text{atan}\left(\frac{\cos(ca)}{\cos(\theta_{6a}).\sin(ca)}\right) \quad \text{if } -\cos(\theta_{6a}).\sin(ca) > 0$$

$$\theta_4 = \text{acos}\frac{\sin(ca).\sin(\theta_6)}{\sigma} + b$$

$$\theta_{4a} = -a\cos\frac{\sin(ca).\sin(\theta_6)}{\sigma} + 2.b$$

$$\theta_{4b} = a\cos\frac{\sin(ca).\sin(\theta_{6a})}{\sigma} + b$$

$$\theta_{4c} = -a\cos\frac{\sin(ca).\sin(\theta_{6a})}{\sigma} + 2.b \quad (13)$$

with : $\sigma = \sqrt{Vx_0^2 + Vz_0^2}$

$$b = -\text{atan}\left(\frac{Vz_0}{Vx_0}\right) - \pi \quad \text{if } Vx_0 < 0$$

$$b = -\text{atan}\left(\frac{Vz_0}{Vx_0}\right) \quad \text{if } Vx_0 > 0$$

Equations (10) to (13) show that angle θ_6 depends on θ_4, that angles θ_4 and θ_5 depend on θ_6. A robot is "resolvable" if a unique solution exists for equation $\theta = f^{-1}(x)$. Our study suggest that our medical robot's wrist is not resolvable.

5.1 Reachable Workspace

Analysis of the resulting equations shows that the determination of the desired current according to a given set of joint variables θ_4, θ_5 and θ_6 is difficult.

Indeed, a given orientation has several solutions for joint variables. Fig. 14 illustrates these points by defining the reachable workspace. The method we propose consists in considering θ_4 as a constant parameter in order to work out joint variables θ_5 and θ_6 according to θ_4. The choice of θ_4 is motivated by optimization method.

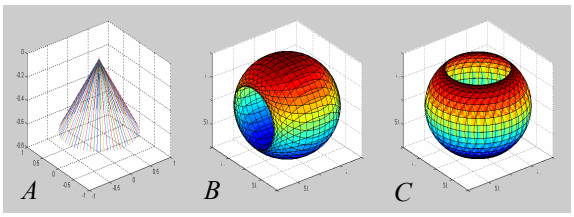

Figure 14: Reachable workspace.

5.2 Control Strategy

The controller must satisfy real time requirements. The sampling frequency is 20 Hz. Moreover, several applications such as artificial vision and data processing take place simultaneously. The controller inputs are :

- Data from artificial vision and image superimposition,
- Desired drill orientation,
- Actual angular values returned by digital encoders.

The algorithm determines the values of V_{xo}, V_{yo}, and V_{zo} that are vector components in the flag reference scorers of the robot. It determines θ_5 and θ_6 with respect to θ_4 and verifies that solutions are in the reachable workspace. If solutions are outside the reachable workspace, the algorithm increments θ_4 with 1° and recalculates θ_5 and θ_6. Incrementation is repeated until a solution is found in the reachable workspace.

6 FURTHER WORKS

The protocol used for identification will be applied in a generic way on the other axes in order to obtain a dynamic model of the robot. As a consequence, we will be able to simulate the robot's dynamic behaviour and to develop safe and efficient control design. On the other hand, our work will concern the following points :

- Accuracy, wrist calibration,
- Study of position / orientation decoupling,
- Trajectory planning, ergonomics.

This medical robot is an invasive and semi-active system. Therefore, an exhaustive study on reliability will also be necessary (Dombre, 2001) before starting clinical simulations and experimentations.

ACKNOWLEDGEMENTS

Authors thank the Doctor DERYCKE, a dental surgeon specialized in implantology, CHIEF EXECUTIVE OFFICER of DENTAL VIEW.

REFERENCES

Langlotz F, Berlemann U, Ganz R, Nolte LP., 2000. Computer-Assisted Periacetabular Osteotomy. Oper. *Techniques in Orthop*, vol 10, N° 1, pp. 14-19

Nikou C, Di Gioia A, Blackwell M, Jaramaz B, Kanade T., 2000. Augmented Reality Imaging Technology for Orthopaedic Surgery. Oper. *Techniques in Orthop*, vol 10, N° 1, pp. 82-86.

Taylor R.,1994. An Image Directed Robotic System for Precise Orthopaedic Surgery. *IEEE Trans Robot*, 10, pp. 261-275.

Lavallee S, Sautot P, Traccaz J, P. Cinquin P, Merloz P., 1995. Computer Assisted Spine Surgery : a technique for accurate transpedicular screw fixation using CT data and a 3D optical localizer. *Journal of Image Guided Surgery*.

Dutreuil J., 2001. Modélisation 3D et robotique médicale pour la chirurgie. *Thèse*, Ecole des Mines de Paris.

Etienne D, Stankoff A, Pennnec X, Granger S, Lacan A, Derycke R., 2000. A new approach for dental implant aided surgery. *The 4th Congresso Panamericano de Periodontologia*, Santiago, Chili.

Granger S., 2003. Une approche statistique multi-échelle au recalage rigide de surfaces : Application à l'implantologie dentaire. *Thèse*, Ecole des Mines de Paris.

Chaumont R, Vasselin E, Gorka M, Lefebvre D., 2005. Robot médical pour l'implantologie dentaire : identification d'un axe, *JNRR05*. Guidel, pp 304-305.

Richalet J., 1998. Pratique de l'identification. Ed. Hermes.

Dombre E., 2001. Intrinsically safe active robotic systems for medical applications. *1st IARP/IEEE-RAS Joint Workshop on Technical Challenge for Dependable Robots in Human Environments*, Seoul, Korea.